

Fluidization in cemented and uncemented granular soils with application to suction-assisted bucket embedment

Pierre Philippe^{1,*}, Abbas Farhat¹, Arsen Abdugaliyev¹, Alexis Doghmane¹, Li-Hua Luu¹, and Pablo Cuéllar^{2,3}

¹INRAE, Aix Marseille Univ., RECOVER, 3275 Route Cézanne, Aix-en-Provence, 13100, France

²BAM, Federal Institute for Materials Research and Testing, Berlin, Germany

³Referat 62 (Dams and Hydraulic constructions), Bayerisches Landesamt für Umwelt, Bürgermeister-Ulrich-Straße 160, Augsburg, 86179, Bavaria, Germany

Abstract. Internal hydraulic flows in granular soils are known for their ability to partially or totally fluidize the material, thus causing a significant loss of mechanical strength. Although this effect is generally undesirable, it can be exploited in certain situations, in particular to facilitate the penetration and anchoring of a bucket-shaped foundation structure in the ground by controlled suction. This type of operation is, however, delicate, with the main risk being the formation of a localized fluidization zone (a phenomenon often called piping or rat-holing) which stops any further penetration of the bucket and may pose a risk to the structure integrity. Using a small-scale physical model built to qualitatively reproduce installation scenarios of foundations for offshore wind turbines, systematic experiments have made it possible to analyze the mechanism of a cylindrical bucket embedment under the effect of suction. Two different types of artificial granular soil are considered: glass beads with and without cementation by solid paraffin bonds. We present here a summary of the results obtained in terms of critical embedment conditions (pressure drop, flow rate) and embedment kinetics (final depth).

1 Context and motivation

The last few decades have seen a sharp increase in the use of suction-assisted foundation techniques as a practical solution for installing offshore structures on the seabed [1-3]. These techniques take advantage of the structure's own weight combined with hydraulic under-pressure induced by a suction flow inside each cylindrical bucket, which will serve as foundation for a mono- or multi-pod structure. Along with the size and geometry of the bucket, the nature of the soil, and particularly its upper layer, is an essential element of the suction installation process, which can potentially prevent the operation from being successful.

The penetration of the bucket induced by a suction flow can indeed stop completely [1, 4, 5], the two main reasons being as follows. First, by gradually increasing the suction pressure, the soil inside the bucket can get fluidized and begin to rise, which can intensify the flow rate in return. There is then a risk that this uplift will reach the upper surface of the bucket, forming a plug of soil and blocking the system before reaching the desired burial depth. Secondly, excessive suction pressure can induce soil erosion in the vicinity of the bucket wall. This fluidization may not be evenly distributed over the entire contact area between the base of the bucket and the ground, but instead be concentrated in one area. Such localized fluidization, often referred to as piping or rat holing, creates a preferential flow path for the suction

flow. This can result in a significant drop in downward driving pressure, which abruptly blocks the penetration process and poses a risk to the integrity of the system.

For sandy soils, which are most frequently encountered in the marine context and may possibly be partially cemented, the precise conditions that can lead to this type of granular fluidization during installation are varied and still poorly understood. There are many influencing parameters, including the properties of the soil (heterogeneity, cementation, etc.), the forces applied (stress state, relative density), but also the exact installation protocol and the stages chosen for the suction procedure (duration, flow rate, etc.).

To better understand these mechanisms on a small scale, it is well suited to use a laboratory scale model allowing more local measurements and observations. In the literature, intermediate- and small-scale physical model tests of bucket installation have been developed, in some cases under centrifuge-increased gravity conditions [6-9]. Following on from these approaches, we have developed a physical model of suction-assisted bucket embedment for experiments on artificial granular soils made of glass beads, with or without internal cementation. We present below our methodology and the main results obtained by systematically varying several of the main control parameters, including critical bucket embedment conditions (differential pressure, suction flow rate) and embedment kinetics (penetration duration, final depth).

* Corresponding author: pierre.philippe@inrae.fr

2 Experimental methodology

2.1 Experimental set-up

The present experiments are based on a small-scale set-up of suction-assisted bucket embedment, developed as a continuation of efforts initiated during the bilateral Franco-German ANR-DFG COMET project (2019-2022). A diagram of our physical model is shown in Figure 1.

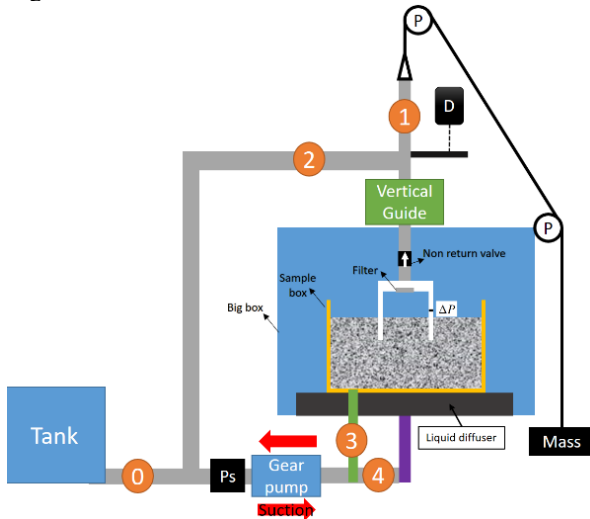


Fig. 1. Diagram of the experimental set-up including the following components: main box, sample box (containing the soil sample to be tested), reservoir tank, bucket with filter, steel tube with vertical guide, gear pump, liquid diffuser, counter-mass, pulleys (P), pressure sensors (ΔP and P_s), displacement sensor (D), non-return valve and other valves numbered from 0 to 4.

The entire device is immersed in a large container with a cross-section of 57.5 cm by 52.7 cm, which holds a sample container (with a square cross-section of 33 cm by 33 cm) containing the soil sample to be tested. A cylindrical box of diameter 10 cm, referred to as the bucket, is initially placed in contact at its open base with the top of the soil sample or can be partially buried in it. The top of the bucket is connected to a vertical steel tube and the whole can be moved along the vertical axis. An upward suction is generated from the steel tube by a gear pump with a maximum flow rate of 32 l/min.

The numbered markers in Figure 1 indicate the several valves in the system which allow the flow direction to be changed during the different stages of the test protocol since the pump can operate in both directions, which is particularly useful for emptying the box after a test. More precisely, once the pump has taken liquid from a reservoir tank (via valve #0) to saturate the sample (via valve #3), fill the main box (via valve #4), and saturate the bucket and the upper pipes (via valves #1 and #2, with the flow temporarily in the opposite direction and thanks to a non-return valve), the hydraulic circuit is closed to operate in a continuous cycle. Note that the flow generated by the incoming pump is homogenized via a diffuser placed beneath the sample box. In addition, a protective filter is fitted at the top of the bucket, at the connection with the steel tube,

to prevent soil particles from entering the gear pump during suction.

A counterweight, weighing up to 5.5 kg, is attached by a system of pulleys to control the partial or even almost total compensation of the combined load of the bucket, the vertical steel pipe and all connected pipes. A camera is placed in front of the bucket to visualize its embedment and the appearance of movement in the tested soil sample. The actual embedment of the bucket over time is measured by a displacement sensor (D in the diagram) monitoring the motion of the vertical steel tube. The differential pressure ΔP generated by the suction in-between both sides of the bucket's lateral wall is measured by two pressure gauges located at mid-height of the wall, one on the outside and the other on the inside. A pressure sensor (P_s) is also placed at the inlet of the gear pump to measure the suction pressure.

2.2 Materials

The granular materials used here are spherical silicate glass beads with three different diameter sizes: 1.40 mm, 2.54 mm and 3.00 mm. For certain experiments, these beads are cemented by solid paraffin bridges with a density of about 880 kg/m³ and a melting temperature around 50°C. The ambient liquid is not water, but a more viscous liquid, in order to induce higher hydrodynamic stresses and thus initiate grain fluidization and bucket penetration into the soil. The mixture in question contains 74% glycerol and 26% distilled water by weight, with a density of 1180 kg/m³ and a dynamic viscosity measured by a falling-ball viscometer as being around 24 times that of water, namely 0.024 Pa/s.

2.3 Sample preparation and test protocols

Two types of artificial granular samples were studied, depending on whether the mono-size set of spherical beads to be tested were cemented together or not. Uncemented bead samples are prepared from a mixture of 15 kg of beads with the addition of 30% by mass of liquid. The whole is poured in the sample box and fully saturated. The initial structure of the sample is prepared in a reproducible manner for each test using a long vertical stick to stir the glass beads in a random and repeated manner. Finally, a ruler is used to level the upper surface. Cemented granular samples are prepared according to the method already presented previously [10], using liquid paraffin to create liquid bridges between the beads, which are then allowed to solidify as they cool. The mass content of paraffin can be varied, modifying the yield adhesive tensile force of a solid bridge. A semi-analytical law has been proposed for this adhesive strength with a quadratic dependence on the bead diameter and a square root dependence on the paraffin volume content [10]. A cemented sample is prepared in two successive layers, each carefully poured into the sample box from a small height to ensure homogeneity. The top surface of the second layer is flattened by a ruler and the whole is left to cool for 12 hours before each experiment.

All the experiments presented here were carried out with a constant suction or by gradually increasing the suction flow rate in small increments (step increase ranging from 0.05 to 0.55 l/min and step duration of approximately 30 s), with the bucket left free to move vertically.

3 Results

3.1 Uncemented granular samples

As shown in Figure 2, when placed on top of the bed and after a small initial penetration before suction, the bucket embeds rather regularly with the increase in suction flow rate until reaching almost the same final depth imposed by the bucket's height. However, higher suction rate is required for full embedment in larger beads, the final flow rate ranging from about 1.2 l/min for the smaller beads to around 3.5 l/min for the larger ones. We note also that embedment is nicely repeatable for the 1.4 mm samples and still acceptable for the two other sizes. Conversely, the differential pressure trends remain very similar whatever the bead size, which is consistent with the fluidization condition of a granular bed. It must also be emphasized that, to achieve these penetrations, it was necessary to partially or fully compensate the static load (here with the maximum counterweight of 5.5 kg). Otherwise the bucket can completely penetrate the granular bed without any suction assistance, particularly for smaller beads.

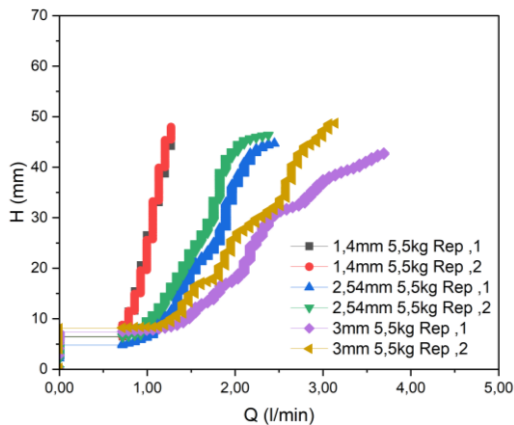


Fig. 2. Bucket embedment with suction flow rate increase for granular samples with the three bead diameters and the maximal counter-mass of 5.5 kg. There are two repetitions for each configuration.

Complementary, the data presented in figure 3, obtained for samples of 3 mm beads, show the kinetics of embedment under constant flow rate condition. As expected, above threshold, higher suction induces an accelerated and slightly deeper embedment. We also logically observe that an increase in the applied load induced by the lightening of the counterweight makes it possible for the bucket to reach a greater depth by requiring lower suction rates. We simultaneously note a substantial increase of the initial penetration prior to suction, associated with a negative pressure drop.

In parallel, some of these results, together with previous tests using a fixed bucket, have been taken as a

benchmark for comparison with simulations based on a combination of DEM and LBM methods [11]. This work is still in progress.

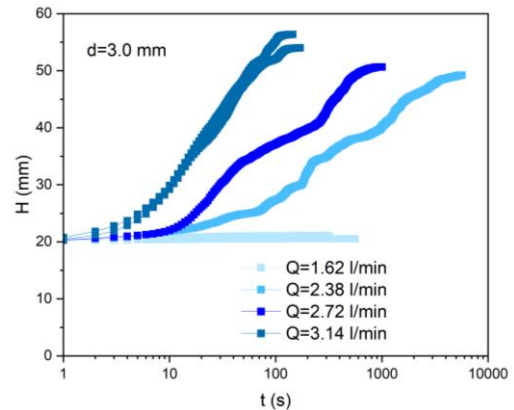


Fig. 3. Bucket embedment at constant suction flow rate for granular samples of diameter 3 mm with the maximal counter-mass of 5.5 kg and with a pre-embedment of 2 cm.

3.2 Cemented granular samples

Several series of data obtained with cemented samples are presented below, in Figure 4 for the 1.4 mm beads and in Figure 5 for the 2.54 mm and 3 mm beads.

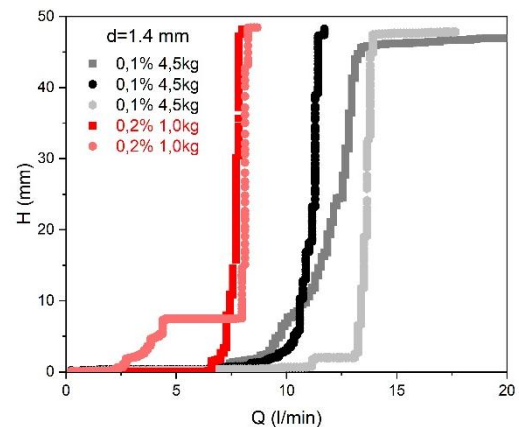


Fig. 4. Bucket embedment with suction flow rate increase for cemented granular samples: bead diameter of 1.4 mm, paraffin content of 0.1% (in black and grey, 3 repetitions) or 0.2% (in red, 2 repetitions) and counter-mass of 4.5 kg (in black and grey) or 1.0 kg (in red).

On these curves, we can observe, in comparison with the granular case, that the reproducibility of the tests is lower and that the suction flow rates necessary for the bucket to penetrate are significantly higher, of about one order of magnitude. It can also be seen that fairly smaller depths are reached for the most cemented samples and/or with the largest balls.

A closer analysis of the penetration kinetics shows that the bucket embedment does not always occur gradually as in uncemented samples, but can involve fairly sudden drops, as a kind of fragile behaviour. This is particularly true for the smallest particles in Fig. 4. Quantitatively, the critical suction rate required to initiate embedment increases substantially with bead diameter, all other parameters being constant, as can be seen by comparing the red curves in Fig. 4, with a

critical flow rate in between 2.5 and 7 l/min, and the green curves in Fig. 5, with a critical flow rate around 16-18 l/min. This trend is mainly due to the hydraulic conductivity of the bed, which increases rapidly with bead diameter, compared to the opposite but more limited effect of grain size on the critical pressure gradient required to separate adhesive bonds.

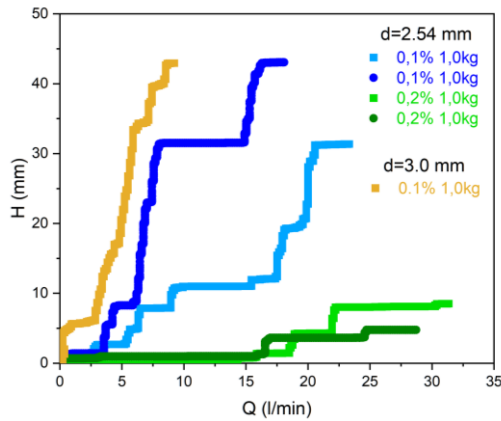


Fig. 5. Bucket embedment with suction flow rate increase for cemented granular samples: bead diameter of 2.54 mm, paraffin content of 0.1% (in blue, 2 repetitions) or 0.2% (in green, 2 repetitions) and counter-mass of 1.0 kg; bead diameter of 3.0 mm, paraffin content of 0.1% and counter-mass of 1.0 kg (in orange).

4 Conclusion and prospects

This experimental work, still at a preliminary stage, has first of all enabled us to validate our physical model of suction-assisted bucket embedment. The results of penetration in granular soil show regular embedment of the bucket, with suction rates and final depth increasing with the size of the grains and decreasing with the static load. The kinetics are more intermittent and erratic in cemented grains, with suction rates that are significantly higher, typically by at least an order of magnitude. Unsurprisingly, samples with large grains and/or a high degree of cementation show better resistance to bucket embedment.

This study is still in progress with a view to obtaining more data and conducting a better quantitative analysis based on both critical pressure drop prediction and introduction of dimensionless numbers derived from fluid mechanics and generalized to the case of cemented grains, as proposed in previous investigations [10, 12].

This work is part of the COMET research project, funded by the Deutsche Forschungsgemeinschaft (DFG grant number 406907912, project ID: CU 393/1-1) and the French Agence Nationale de la Recherche (ANR grant number ANR-2018-CE92-0007), whose supports are gratefully acknowledged.

References

1. H. Sturm, Design Aspects of Suction Caissons for Offshore Wind Turbine Foundations, in Proceedings of 19th International Conference on

- Soil Mechanics and Geotechnical Engineering, Seoul, Korea, September 17-21 (2017)
2. X. Wu, Y. Hu, Y. Li, J. Yang, L. Duan, T. Wang, T. Adcock, Z. Jiang, Z. Gao, Z. Lin, A. Borthwick and S. Liao, Foundations of offshore wind turbines: A review. *Renewable and Sustainable Energy Reviews* **104**, 379 (2019) <https://doi.org/10.1016/j.rser.2019.01.012>.
3. S. Kay, S. Gourvenec, E. Palix and E. Alderlieste, Intermediate Offshore Foundations (1st ed.), (CRC Press, 2021)
4. O. Harireche, M. Mehravar and A. M. Alani, Suction caisson installation in sand with isotropic permeability varying with depth. *Applied Ocean Research* **43**, 256 (2013) <https://doi.org/10.1016/j.apor.2013.10.008>.
5. B.-F. Chen and T.-T. Huang, On fluid-filled mixture model for suction pile foundation analysis. *Ocean Engineering* **188**, 106306 (2019) <https://doi.org/10.1016/j.oceaneng.2019.106306>.
6. J. H. Kim, S. T. Lee and D. S. Kim, Observation of sand movement during bucket installation. *International Journal of Physical Modelling in Geotechnics* **19(1)**, 1 (2019) <https://doi.org/10.1016/j.jphmg.16.00048>.
7. B. Bienen, R. T. Klinkvort, C. D. O'Loughlin, F. Zhu and B. W. Byrne, Suction caissons in dense sand, part I: installation, limiting capacity and drainage. *Géotechnique* **68(11)**, 937 (2018) <https://doi.org/10.1016/j.jgeot.16.P.281>.
8. A. K. Koterias and L. B. Ibsen, Medium-scale laboratory model of mono-bucket foundation for installation tests in sand. *Canadian Geotechnical Journal* **56(8)**, 1142 (2020) <https://doi.org/10.1139/cgj-2018-0134>.
9. R. Ragni, B. Bienen, S. Stanier, C. O'Loughlin and M. Cassidy, Observations during suction bucket installation in sand. *International Journal of Physical Modelling in Geotechnics* **20(3)**, 132 (2020) <https://doi.org/10.1016/j.jphmg.18.00071>.
10. A. Farhat, L.-H. Luu, A. Doghmane, P. Cuéllar, N. Benahmed, T. Wichtmann and P. Philippe, Micro and macro mechanical characterization of artificial cemented granular materials. *Granular Matter* **26**, 65 (2024) <https://doi.org/10.1007/s10035-024-01426-2A>.
11. S. Kemmler, P. Cuéllar, A. Artinov, L.-H. Luu, A. Farhat, P. Philippe, C. Rettinger and H. Köstler, A fully-resolved micromechanical simulation of piping erosion during a suction bucket installation. *Computers and Geotechnics* (under review)
12. A. Farhat, P. Philippe, L.-H. Luu, A. Doghmane and P. Cuéllar, Hydraulic failure of granular materials with artificial cementation. *Phys. Rev. Fluids* **9**, 064305 (2024) <https://doi.org/10.1103/PhysRevFluids.9.064305>.